Electronic Supplementary information for "Resonant scattering enhanced photothermal microscopy"

Qiang Li,[a] Zhonghong Shi,[a] Lijun Wu,*[,a] Hong Wei,*[,b,c]

[a] *Guangdong Provincial Key Laboratory of Nanophotonic Functional Materials and Devices, School of Information and Optoelectronic Science and Engineering, South China Normal University, Guangzhou 510006, China. E-mail: ljwu@scnu.edu.cn*

[b] *Institute of Physics, Chinese Academy of Sciences, Beijing 100190, China. E-mail: weihong@iphy.ac.cn*

[c] *Songshan Lake Materials Laboratory, Dongguan 523808, China*

1. Experimental details

The gold NRs used in this study were prepared by a wet chemical method involving seed mediated growth in the presence of silver.[1] Figure S1a shows the UV–Vis extinction spectrum of the gold NRs in water. The spectrum is characterized by two bands. The shorter wavelength band (~515 nm) is attributed to the transverse surface plasmon resonance mode, and the longer wavelength band (~702 nm) is attributed to the longitudinal surface plasmon resonance mode. Figure S1b shows the transmission electron microscope (TEM) image of the gold NRs. The diameters of the gold NRs are about 20 nm and the lengths are broadly distributed in the range of 30-70 nm (Figure S1c,d).

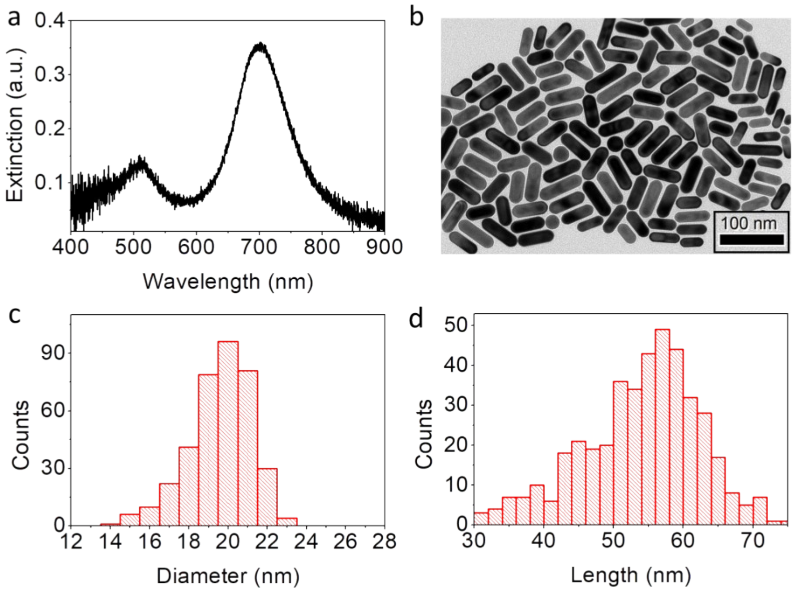

Figure S1. (a) UV–Vis extinction spectrum of the gold NRs in water. (b) TEM image of the gold NRs. (c) Statistics of the diameter of the gold NRs. (d) Statistics of the length of the gold NRs.

The prepared gold NRs were firstly spin-coated on top of the piranha solution cleaned glass coverslips. Then PVA solutions with concentration of 2.1wt%, 3.1wt%, and 3.1wt% were spin-coated on top of three glass coverslips as the surrounding medium of the gold NRs with spin-coating speed of 1500, 2800, and 1400 r/min, respectively. In order to measure the thickness of the PVA film, the PVA films were scratched with a sharp stick and the step heights were measured using an atomic force microscope (AFM, NanoWizard 4, JPK Instruments AG). The roughness of the PVA film was found to be less than 5 nm. The measured thicknesses of the three PVA films are about 50, 80 and 100 nm, respectively (Figure S2).

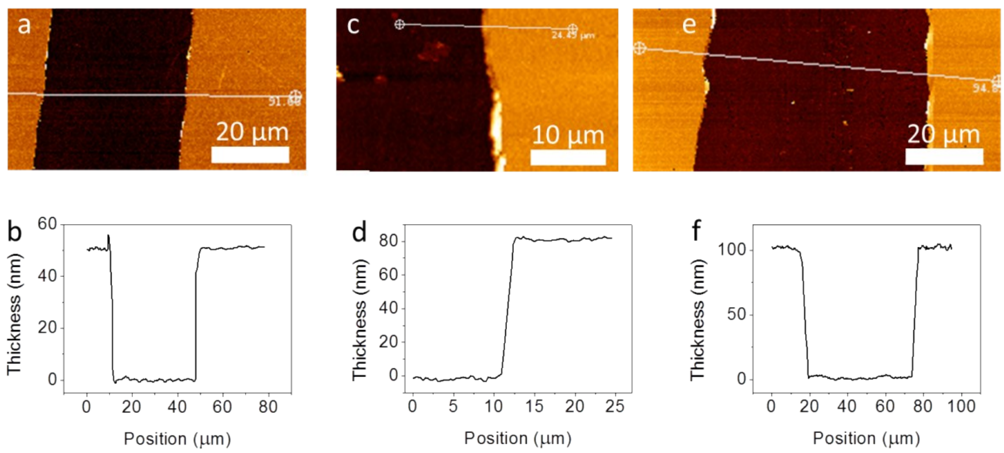

Figure S2. (a,c,e) AFM images of the scratch borders on three glass coverslips. (b,d,f) Measured height profiles across the scratches. The measured thicknesses of the three PVA films are about 50 (a,b), 80 (c,d), and 100 nm (e,f), respectively.

The PT microscope was built based on an inverted microscope (IX 73, Olympus) equipped with a 100× oil immersion objective with NA of 0.9 (UPLFLN100×OI2, Olympus). After passing through the AOM (CNI) with a typical modulation frequency of 80 kHz, the heating laser beam of 532 nm wavelength (MGL-DS-532, CNI) was expanded by a telescope system and then overlaid with the probe beam of 730 nm wavelength (OBIS-LX-730, Coherent). The two collimated beams were focused onto the same spot at the sample surface. The widths of the focal spots are about 0.5 and 1.0 μm for the heating beam and probe beam, respectively. The iSCAT light, including the scattering light from the gold NR and the reference light reflected at the sample interface, passed through an interference filter to block the heating laser light and was then directed to an avalanche photodiode (APD410A, Thorlabs) through a spatial filter system. The PT signal, which is the intensity variation of the iSCAT light induced by the modulated heating laser beam, was obtained using a lock-in amplifier (MFLI-5MHz, Zurich Instruments) that was in phase referenced to the frequency of AOM. The PT images were recorded by scanning the sample over the fixed laser spots by means of a piezo-scanner with a step size of 41 nm. The incident power of heating beam and probe beam were 0.72 mW and 3 μW, respectively. The heating beam and the probe beam were circularly polarized and linearly polarized, respectively, in all the measurements. The dark-field scattering spectra were measured on the same setup. The unpolarized white light generated by a halogen lamp was focused onto the sample by a dark-field condenser and the light scattered by the gold NR was collected by the objective and recorded by a spectrometer equipped with an electron-multiplying charge coupled device (DU970N-BV, Andor).

2. The optical and thermal parameters for the selected materials

The complex permittivity of gold NRs was taken based on the values measured by Johnson and Christy for bulk gold.[2]

Table S1. Optical and thermal parameters for selected materials at optical wavelength of 730 nm (room temperature and normal pressure).[3, 4]

	Real part of permittivity ε'	Imaginary part of permittivity ε''	$\frac{\partial \varepsilon'}{\partial T}$	$\frac{\partial \varepsilon''}{\partial T}$	Heat capacity [$Jkg^{-1}K^{-1}$]	Thermal conductivity [$Wm^{-1}K^{-1}$]	Density [kg/m^3]
Gold	-18.657	1.146	$1.550 \cdot 10^{-2}$	$4.300 \cdot 10^{-3}$	385	397	8933
PVA	2.167	0	$-5.888 \cdot 10^{-4}$	0	1334	0.22	1190
Glass	2.310	0	$3.800 \cdot 10^{-5}$	0	853	1.05	2520

3. The influence of probe beam on the rise of temperature on the gold NR

According to the power and the focal spot size provided in Section 1, the ratio between the power density of the heating beam and probe beam is 960. Figure S3 shows the simulated absorption spectra of gold NR when the incident light is polarized parallel and perpendicular to the long axis of the NR. The longitudinal surface plasmon resonance wavelength of the gold NR is 730 nm. In experiment, the heating beam was circularly polarized and the probe beam was linearly polarized parallel to the long axis of the NR. The ratio between the absorption cross-section at 532 nm (heating beam wavelength) and 730 nm (probe beam wavelength) is about 1/20. Thus the ratio between the absorbed power of gold NR at the heating and probe beam wavelengths is 48. Since the rise of temperature on gold NR is proportional to the absorbed power, the rise of local temperature induced by the probe beam is 48 times less than that induced by heating beam.

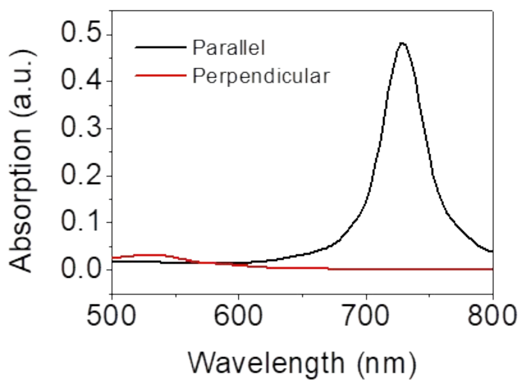

Figure S3. The absorption spectra of gold NR when the incident light is polarized parallel (black line) and perpendicular (red line) to the long axis of the NR. The longitudinal surface plasmon resonance wavelength is 730 nm.

4. The relationship between the sign of PT signal and the longitudinal surface plasmon resonance wavelength of gold NRs

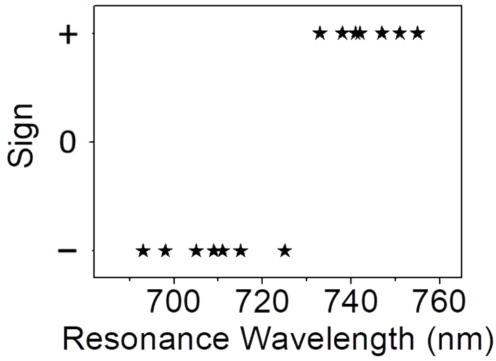

Figure S4. Distribution of the sign of PT signal as a function of the resonance wavelength for the 15 gold NRs marked by green circles in Figure 2b. We found that the resonance wavelength λ_{res} of gold NR with positive PT signal is longer than that of gold NR with negative PT signal.

5. The normalized PT signal as a function of the resonance wavelength for gold NRs covered by PVA film with thickness of 80 nm

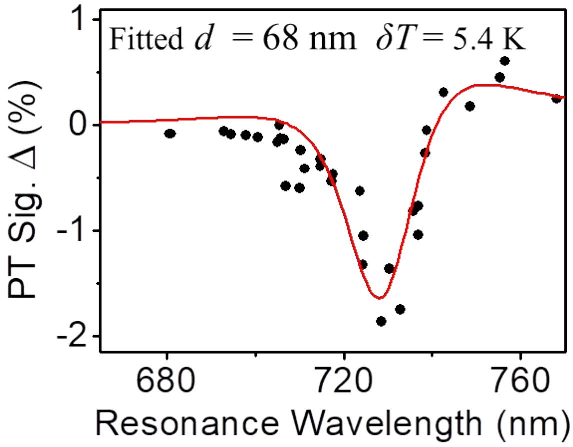

Figure S5. Normalized PT signal Δ as a function of the resonance wavelength λ_{res} of gold NRs. The thickness of the PVA film is 80 nm. The red solid line represents the theoretical fit of the normalized PT signal according to eq 2. The fitted thickness of PVA film d and rise of local temperature δT are provided.

6. The theoretical description of the iSCAT signal

Let $\vec{E}_{\mathrm{i}}$ denote the electric field of the probe laser light at wavelength λ seen by the gold NR in the focus of the microscope objective without heating beam. The scattering field at the detector is given by $\vec{E}_{\mathrm{scat}} = \eta\alpha\vec{E}_{\mathrm{i}}$, where η takes into account the detection efficiency and $\alpha = |\alpha| e^{i\phi_{\mathrm{scat}}}$ is the complex polarizability of the gold NR carrying information on amplitude ($|\alpha|$) and phase difference (ϕ_{scat}) between the scattering field ($\vec{E}_{\mathrm{scat}}$) and the driving field ($\vec{E}_{\mathrm{i}}$). At the same time, the incident probe light undergoes reflection at the sample interfaces (the reflection almost entirely originates at the PVA-air interface because of the very close refractive index of PVA and glass), giving rise to the reference field $\vec{E}_{\mathrm{ref}} = r\vec{E}_{\mathrm{i}} e^{-i\pi(1/2 - 4dn/\lambda)}$ at the detector, where d and n are the thickness and refractive index of the PVA film, respectively, r is a real quantity taking into account the effective field reflectivity for the focused probe beam, the phase of -π/2 has been introduced to account for the Gouy phase shift that is accumulated by the reflected Gaussian beam with respect to $\vec{E}_{\mathrm{i}}$,[5] and the phase shift of $4\pi dn/\lambda$ is added by the PVA film. Because the reference light and the scattering light have similar field distributions at the detector, the detected intensity of their interferometric field in the absence of heating beam illumination can be expressed as the eq 1 in the main text.

7. The dependence of local temperature on gold NR length upon heating beam illumination

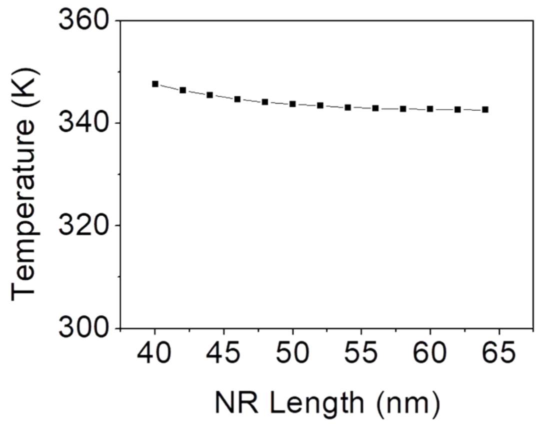

Figure S6. The simulated temperature on gold NR as a function of its length. The gold NR is 20 nm in diameter. The heating light of 532 nm wavelength is circularly polarized and the power is 2.5 mW. Because the absorption cross-section of gold NR at the wavelength of 532 nm is not much size-dependent, the rise of local temperature is little changed and assumed to be the same for NRs with different lengths.

8. Theoretical fitting of the normalized PT signal

Let's consider the simple case of a gold spheroid embedded in uniform PVA medium. The gold spheroid has two short axes of equal length (diameter) $a=b$ and a long axis of length c. The aspect ratio is $R=c/a$. For polarization of incoming light parallel to the long axis of the gold spheroid, the polarizability is given as: [6]

$$\alpha=\frac{\varepsilon_0 V\left(\varepsilon-\varepsilon_{\mathrm{m}}\right)}{\varepsilon_{\mathrm{m}}+L\left(\varepsilon-\varepsilon_{\mathrm{m}}\right)}, \tag{S1}$$

where $V=\left(4\pi/3\right)abc$ is the volume of the gold spheroid, and $\varepsilon=\varepsilon'+i\varepsilon''$ and ε_{m} are the permittivities of the gold spheroid and its surrounding PVA medium, respectively. The geometrical factor L is given by:

$$L=\frac{1-e^2}{e^2}(-1+\frac{1}{2e}\ln\frac{1+e}{1-e}),\quad e^2=1-\left(\frac{a}{c}\right)^2. \tag{S2}$$

Figure S7a displays the calculated amplitude of polarizability $|\alpha|$ of gold spheroid with aspect ratio of 3 (the diameter is 10 nm) as a function of optical wavelength. The peak position of the polarizability, corresponding to the longitudinal surface plasmon resonance wavelength λ_{res}, is 717 nm.

The longitudinal surface plasmon resonance condition is roughly fulfilled when the denominator of eq S1 vanishes, or when [7]

$$\varepsilon'=\frac{L-1}{L}\varepsilon_{\mathrm{m}}\ . \tag{S3}$$

A plot of ε' as a function of optical wavelength λ in the range between 650 and 810 nm is found to be nearly linear (Figure S7b), and a fit gives the following values for the intercept and slope

$$\varepsilon'=35.230-0.074\lambda\ . \tag{S4}$$

Similarly, plotting $\left(L-1\right)/L$ as a function of the aspect ratio R (Figure S7c) and linear fitting yield

$$\frac{L-1}{L}=3.130-3.788R\ . \tag{S5}$$

Combining eqs S3-5 gives

$$\lambda_{\mathrm{res}}=476.08-(42.30-51.19R)\varepsilon_{\mathrm{m}}\ . \tag{S6}$$

Eq S6 is plotted in Figure S7d as the green line, which shows very good agreement with the resonance wavelength calculated by using the full expression of eq S1 (black line in Figure S7d).

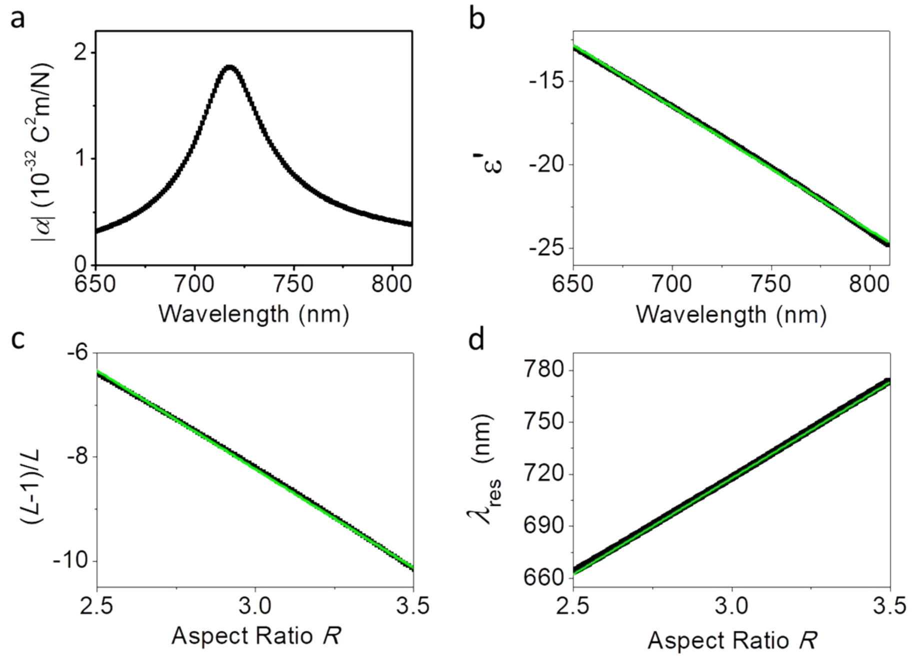

Figure S7. (a) Amplitude of polarizability $|\alpha|$ for incoming light of different wavelength polarized parallel to the long axis of gold spheroid with aspect ratio of 3 (the diameter is 10 nm). (b) Real part of the permittivity of gold ε' as a function of the optical wavelength (black dot line). The green solid line represents the linear fitting of the data. (c) Value of $(L-1)/L$ as a function of the aspect ratio R (black dot line). The green solid line represents the linear fitting of the data. (d) Resonance wavelength λ_{res} of the gold spheroid as a function of its aspect ratio R obtained by using the full expression of eq S1 (black dot line) and plotted according to eq S6 (green solid line).

The TL around the heated gold NR can be simply treated as the coated shell with thickness of s around the heated gold spheroid. We denote by ε_1 the permittivity of the inner core spheroid which has two short axes of equal length $a_1 = b_1 = a = b$ and a long axis of length $c_1 = c$. ε_2 is the permittivity of the outer shell, and the core-shell spheroid has two short axes of equal length $a_2 = b_2 = a_1 + s$ and a long axis of length $c_2 = c_1 + s$. The core-shell spheroid is in uniform PVA medium with permittivity ε_{m}. For polarization of incoming light parallel to the long axis of the core-shell spheroid, the polarizability is given as:[6]

$$\alpha' = \frac{\varepsilon_0 V_2\left(\left(\varepsilon_2-\varepsilon_{\mathrm{m}}\right)\left[\varepsilon_2+\left(\varepsilon_1-\varepsilon_2\right)\left(L_3^1-fL_3^2\right)\right]+f\varepsilon_2\left(\varepsilon_1-\varepsilon_2\right)\right)}{\left(\left[\varepsilon_2+\left(\varepsilon_1-\varepsilon_2\right)\left(L_3^1-fL_3^2\right)\right]\left[\varepsilon_{\mathrm{m}}+\left(\varepsilon_2-\varepsilon_{\mathrm{m}}\right)L_3^2\right]+fL_3^2\varepsilon_2\left(\varepsilon_1-\varepsilon_2\right)\right)}, \quad \text{(S7)}$$

where $V_2=(4\pi/3)a_2b_2c_2$ is the volume of the core-shell spheroid, $f=(a_1b_1c_1)/(a_2b_2c_2)$ is the fraction of the total particle volume occupied by the inner spheroid, and L_3^1 and L_3^2 are the geometrical factors for the inner and outer spheroids, respectively:

$$L_3^{\mathrm{k}} = \frac{1-e^2}{e^2}\left(-1+\frac{1}{2e}\ln\frac{1+e}{1-e}\right), \quad e^2 = 1-\left(\frac{a_{\mathrm{k}}}{c_{\mathrm{k}}}\right)^2 \quad (\mathrm{k}=1,2). \quad \text{(S8)}$$

Based on the simulated local temperature distribution around the heated gold NR (Figure 4a), the thickness of the heat induced "shell" is set as s = 25 nm. The temperature of the core-shell spheroid is assumed to be δT above the room temperature of 300 K. The permittivities of the heated gold spheroid and its shell are $\varepsilon_1=\varepsilon+\frac{\partial\varepsilon}{\partial T}\delta T$ and $\varepsilon_2=\varepsilon_{\mathrm{m}}+\frac{\partial\varepsilon_{\mathrm{m}}}{\partial T}\delta T$, respectively, where $\frac{\partial\varepsilon}{\partial T}=\frac{\partial\varepsilon'}{\partial T}+i\frac{\partial\varepsilon''}{\partial T}$ and $\frac{\partial\varepsilon_m}{\partial T}$ can be obtained from the thermo-optic coefficient of gold and PVA (Table S1). We fitted the data of normalized PT signal shown in Figure 3a,b, and Figure S5 by using the eqs S1, S6, S7, and eq 2 in the main text with η/r, d and δT left as free fitting parameters

9. The contribution of intensity of pure scattering light from gold NR to the normalized PT signal

The normalized PT signal with ($\Delta_{\mathrm{w/}}$) and without ($\Delta_{\mathrm{w/o}}$) the contribution of intensity of pure scattering light from gold NR can be expressed as:

$$\Delta_{\mathrm{w/}} = 2\frac{\eta}{r}\left(|\alpha'|\cos\phi'-|\alpha|\cos\phi\right)+\left(\frac{\eta}{r}\right)^2\left(|\alpha'|^2-|\alpha|^2\right), \quad \text{(S9)}$$

and

$$\Delta_{\mathrm{w/o}} = 2\frac{\eta}{r}\left(|\alpha'|\cos\phi'-|\alpha|\cos\phi\right), \quad \text{(S10)}$$

respectively. Based on the fitted parameters of Figure 3a in the main text, we plotted the PT signal with (red lines) and without (green lines) the contribution of intensity of pure scattering light from gold NR with different resonance wavelength (Figure S8). Clearly, the difference between $\Delta_{\mathrm{w/}}$ and $\Delta_{\mathrm{w/o}}$ is so small that the term proportional to $(\eta/r)^2$ in eq S9 can be ignored.

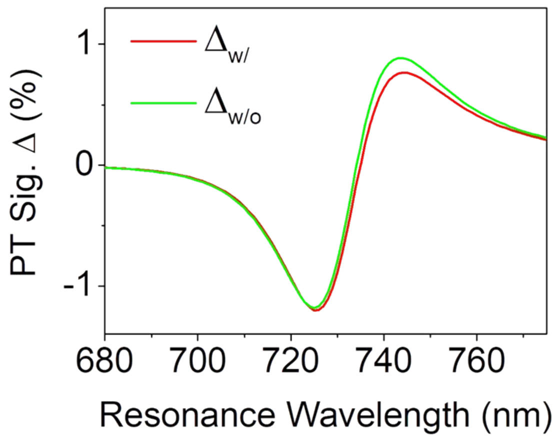

Figure S8. Normalized PT signal with (red lines) and without (green lines) the contribution of intensity of pure scattering light from the gold NR with different resonance wavelength.

10. The phase shift of the scattering field as a function of the resonance wavelength of gold NR

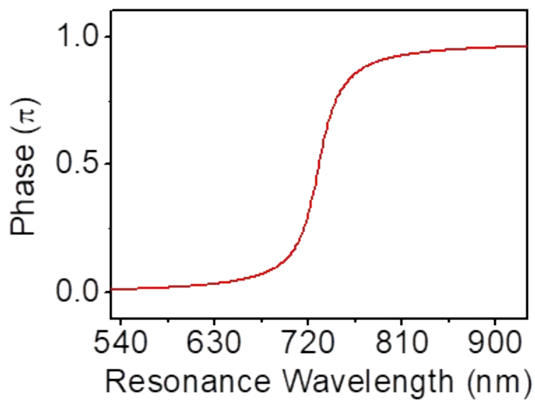

Figure S9. The phase difference between the scattering field and the driving field ϕ_{scat} as a function of the resonance wavelength of gold NR. The scattering field from the gold NR experiences a transition from in phase ($\phi_{scat} = 0$) to out of phase ($\phi_{scat} = \pi$) with the driving field when the resonance wavelength λ_{res} scans across the probe light wavelength of 730 nm.

11. Heat induced variation of polarizability amplitude and phase difference

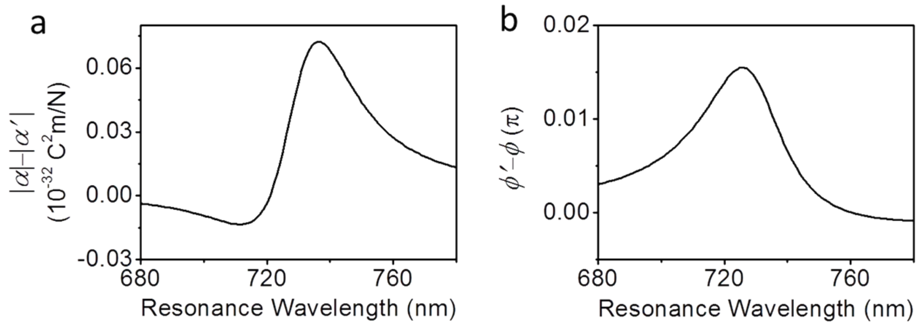

Figure S10. The heat induced variation of polarizability amplitude $|\alpha|-|\alpha'|$ (a) and phase difference $\phi'-\phi$ (b). Clearly, the variation is more obvious for gold NR near resonant with the probe light compared with the non-resonant gold NR. The data is obtained from Figure 3c of main text.

12. The polarizability of gold NR in TL

Based on the extracted parameters of Figure 3b, we calculated the normalized PT signal as a function of the resonance wavelength of gold spheroid with diameter of 20, 5, 3 nm, respectively. The black dot lines in Figure S11 show the obtained PT signal when the polarizability of gold NR in TL is treated as that of the core-shell shaped spheroid. The TL induced shell is 25 nm in thickness. The red lines show the PT signal when the polarizability of gold NR in TL is simply treated as that of gold spheroid embedded in the uniform medium with permittivity of TL. For the gold spheroid with diameter of 20 nm (Figure S11a), the black dot line and red line are almost coincident, which means that the polarizability of gold NR in TL is nearly the same as that of gold NR embedded in the uniform medium with permittivity of TL. For the gold spheroid with diameter of 5 nm and 3 nm (Figure S11b,c), the black dot lines and red lines are a little separated and the separation is more obvious for gold spheroid with smaller diameter. Our result indicates that the scattering field from the gold NR in TL near the longitudinal surface plasmon resonance condition is governed by the inside gold NR and the contribution from the heat induced dielectric TL (shell) can be ignored, which is valid for gold NR with diameter as small as 5 nm. Thus the PT signal of gold NR with resonance wavelength around the wavelength of probe light is mainly caused by the heat induced variation of the polarizability of the gold NR.

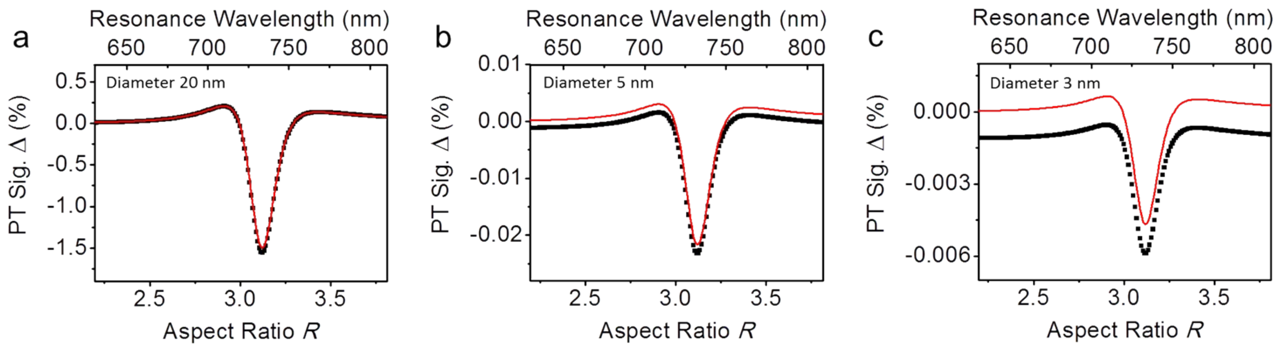

Figure S11. (a-c) Normalized PT signal as a function of the aspect ratio R of the gold spheroid with diameter of 20 nm (a), 5 nm (b), and 3 nm (c). The black dot lines show the obtained PT signal when the polarizability of gold NR in TL is treated as that of core-shell shaped spheroid. The red lines show the PT signal when the polarizability of gold NR in TL is simply treated as that of gold spheroid embedded in the uniform medium with permittivity of TL.

12. The influence of local temperature on the polarizability of gold NR

Considering the gold spheroid with aspect ratio of R embedded in the surrounding PVA medium which is δT above the room temperature of 300 K, the permittivities of the gold and PVA are given by:

$$\varepsilon'(\lambda,\delta T)=35.230-0.074\lambda+\frac{\partial\varepsilon'}{\partial T}\delta T\,, \qquad \text{(S11)}$$

and

$$\varepsilon_{\mathrm{m}}(\delta T)=2.167+\frac{\partial\varepsilon_{\mathrm{m}}}{\partial T}\delta T\,, \qquad \text{(S12)}$$

respectively. The longitudinal surface plasmon resonance condition is roughly fulfilled when the denominator of eq S1 vanishes (corresponding to eq S3), which gives the resonance wavelength λ_{res} of the gold spheroid as follows:

$$\lambda_{\mathrm{res}}(\delta T)=384.42+110.93R+\left[13.51\frac{\partial\varepsilon'}{\partial T}-(42.30-51.19R)\frac{\partial\varepsilon_{\mathrm{m}}}{\partial T}\right]\delta T\,. \qquad \text{(S13)}$$

The derivative versus temperature of the resonance wavelength can be expressed as:

$$\frac{\partial\lambda_{\mathrm{res}}}{\partial T}=13.51\frac{\partial\varepsilon'}{\partial T}-(42.30-51.19R)\frac{\partial\varepsilon_{\mathrm{m}}}{\partial T}\,. \qquad \text{(S14)}$$

The amplitude of the polarizability at resonance wavelength $|\alpha|_{\mathrm{res}}$ can be approximated as:

$$|\alpha|_{\mathrm{res}} \approx \frac{\varepsilon_0 V}{L^2}\frac{\varepsilon_{\mathrm{m}}}{\varepsilon''}. \tag{S15}$$

Therefore, the derivative versus temperature of $|\alpha|_{\mathrm{res}}$ can be given by:

$$\frac{\partial|\alpha|_{\mathrm{res}}}{\partial T} \approx \frac{\varepsilon_0 V}{L^2}\frac{1}{\varepsilon''}\left[\frac{\partial\varepsilon_{\mathrm{m}}}{\partial T} - \frac{\varepsilon_{\mathrm{m}}}{\varepsilon''}\left(\frac{\partial\varepsilon''}{\partial T} + \frac{\partial\varepsilon''}{\partial\lambda}\frac{\partial\lambda_{\mathrm{res}}}{\partial T}\right)\right]. \tag{S16}$$

The derivative of $|\alpha|_{\mathrm{res}}$ is determined by two factors. One is the temperature derivative of the permittivity $\partial\varepsilon_{\mathrm{m}}/\partial T$ and $\partial\varepsilon''/\partial T$. The other one is the variation of the permittivity ε'' induced by the shift of resonance wavelength which is provided by eq S14.

For gold spheroid (diameter of 20 nm) with resonance wavelength λ_{res} in the interesting range around 730 nm, the aspect ratio R is about 3.12 and $\partial\varepsilon''/\partial\lambda \approx 4.49\times 10^{-3}$. Figure S12a,b present the temperature induced variation of resonance wavelength $\delta\lambda_{\mathrm{res}}$ and amplitude of the polarizability at resonance wavelength $\delta|\alpha|_{\mathrm{res}}$ according to eq S14 and S16. The contributions from the temperature derivative $\partial\varepsilon_{\mathrm{m}}/\partial T$, $\partial\varepsilon'/\partial T$ and $\partial\varepsilon''/\partial T$ are also plotted separately. With the rise of local temperature, the decrease of $|\varepsilon'|$ and ε_{m} result in the red shift and blue shift of λ_{res}, respectively. After taking the thermo-optic parameters of gold and PVA, we found that $\partial\lambda_{\mathrm{res}}/\partial T$ is positive, indicating the resonance wavelength λ_{res} is red-shifted at higher temperature. Because the polarizability of a gold NR reaches the maximum at the surface plasmon resonance wavelength, the red shift of the resonance wavelength results in the left shift of the polarizability at the probe light wavelength as a function of the resonance wavelength as shown in Figure 3c. The decreased ε_{m} and $|\varepsilon'|$, and the increased ε'' at higher temperature all result in the reduction of $|\alpha|_{\mathrm{res}}$, and the contribution from the temperature induced increase of ε'', corresponding to the enhancement of electron scattering in gold, is dominant.

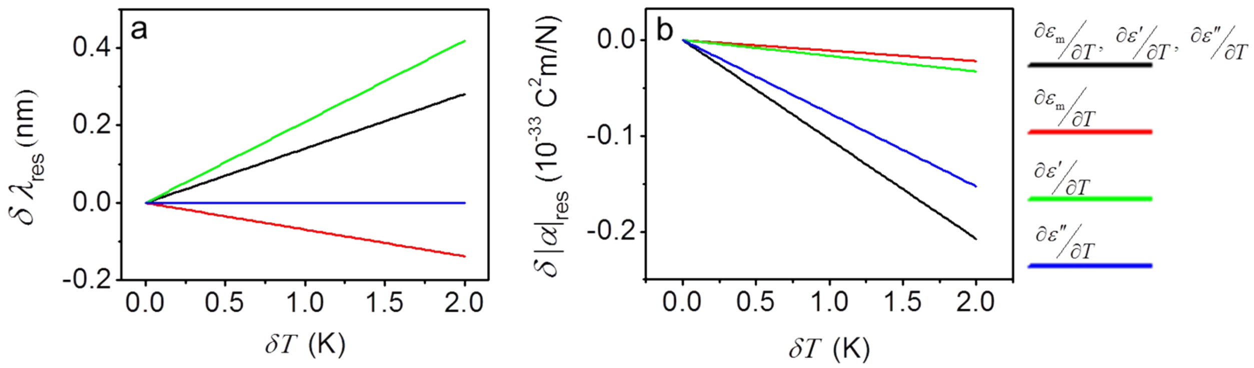

Figure S12. The variation of resonance wavelength $\delta\lambda_{res}$ (a) and amplitude of polarizability at optical resonance wavelength $\delta|\alpha|_{res}$ (b) as a function of the rise of environment temperature δT above room temperature of 300 K (black lines). The contribution from $\partial\varepsilon_m/\partial T$ (red lines), $\partial\varepsilon'/\partial T$ (green lines), and $\partial\varepsilon''/\partial T$ (blue lines) are also plotted separately.

14. The dependence of PT signal on the thickness of PVA film

For small rise of local temperature δT, the normalized PT signal of eq 2 in the main text can be rewritten as:

$$\begin{aligned}\Delta &= 2\frac{\eta}{r}\left(\frac{\partial|\alpha|}{\partial T}\cos\phi - \frac{\partial\phi_{scat}}{\partial T}|\alpha|\sin\phi + \frac{\eta}{r}|\alpha|\frac{\partial|\alpha|}{\partial T}\right)\delta T \\ &= 2\frac{\eta}{r}\delta T\left(A\sin\left(\phi_{scat} + \pi\left(1/2 - 4dn/\lambda\right) + c\right) + \frac{\eta}{r}|\alpha|\frac{\partial|\alpha|}{\partial T}\right),\end{aligned} \tag{S17}$$

where $A = \sqrt{\left(\frac{\partial|\alpha|}{\partial T}\right)^2 + \left(\frac{\partial\phi_{scat}}{\partial T}|\alpha|\right)^2}$ and c satisfies $\cos c = -\frac{\partial\phi_{scat}}{\partial T}\frac{|\alpha|}{A}$ and $\sin c = \frac{\partial|\alpha|}{\partial T}\frac{1}{A}$. This equation indicates that the normalized PT signal periodically oscillates as a function of the thickness d of the PVA film. Figure S13a presents the normalized PT signal Δ of gold NRs with different resonance wavelength λ_{res} as a function of the thickness of the PVA film plotted according to eq 2. As can be seen, for a gold NR with a certain resonance wavelength λ_{res}, the PT signal oscillates with the increased thickness d of PVA film which linearly changes the phase difference between the scattering field and the reference field. The maximum amplitude of the PT signal is obtained for gold NR with resonance wavelength around 730 nm (Figure S13b), in accordance with the wavelength of probe laser light.

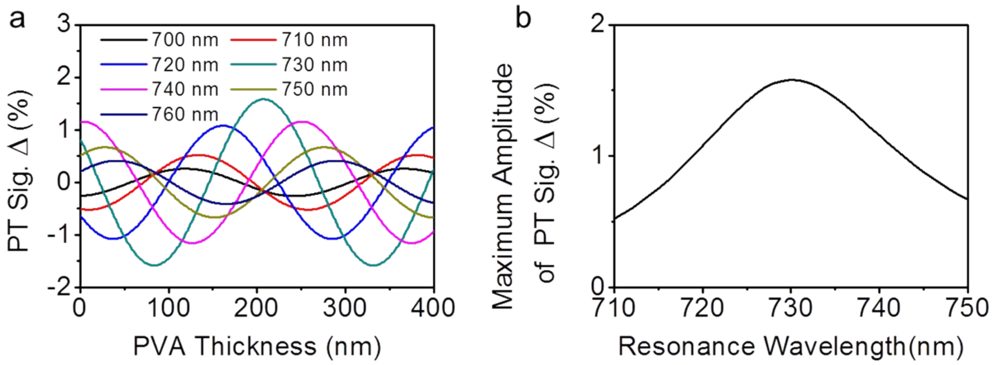

Figure S13. (a) Normalized PT signal Δ of gold NRs with resonance wavelength λ_{res} of 700, 710, 720, 730 ,740, 750, and 760 nm as a function of the thickness of the PVA film. (b) The maximum amplitude of the PT signal as a function of the resonance wavelength of gold NRs

15. Simulation details

The three-step simulations were performed by combining the “Wave Optics-Frequency Domain” module and “Heat Transfer” module in a finite-element method based commercial software (COMSOL Multiphysics). The gold NR was modeled as a cylinder capped with a hemisphere at each end. The PVA film in our simulation is 50 nm in thickness. The diameter of the NR is 20 nm. The beam waist of the heating (wavelength of 532 nm) and probe (wavelength of 730 nm) Gaussian beam are 0.5 and 1.0 μm, respectively. The first step in the simulation was to calculate the ohmic loss caused by the heating laser, which is a full wave electromagnetic simulation. A port boundary condition was used to define the heating Gaussian beam and the corresponding incident power. In the second step, the ohmic loss generated above was used as the heat source to simulate the heating process. Here we consider the heating process as a time-dependent problem. We set the heating time to 50 μs to ensure that the system is close to equilibrium. We used the infinite-domain boundary condition to simulate the infinite outer space. The initial and the ambient temperature was set to 300 K. In the last step, a probe Gaussian beam was applied to obtain the near field of iSCAT probe light before and after the rise of local temperature. The near field distribution of the iSCAT probe light was decomposed into a series of far field plane waves propagating at different directions. Any plane waves inside the collection angle of the objective were then re-focused onto the image plane of the objective where the electric field was analyzed. The reflection field from the sample interface (that is, the reference field) was obtained when the probe Gaussian beam was focused onto the glass-PVA film interface without gold NR. By using the electric field differential method, pure scattering field from the gold NR can be obtained. The phase difference between the pure scattering field and the reference field is obtained in the far field region.

16. The simulated temperature around the heated gold NR

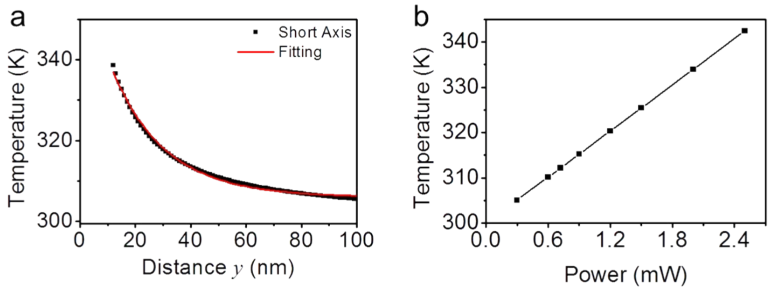

Figure S14. (a) Enlarged temperature profile along the short axis of the gold NR in Figure 4b of the main text. The red solid line represents the fitting of the data using the equation "$T = A_1\exp(-y/L_1)+T_0$". The fitted result of L_1 is 21 nm. (b) Temperature on the gold NR as a function of the power of heating beam.

17. The response of PT signal to the variation of local refractive index

The black lines in Figure S15a,b show the normalized scattering spectrum and absorption spectrum of a gold spheroid embedded in PVA medium. The gold spheroid is 18 nm in length and 5 nm in diameter. Both of the scattering intensity and the absorption intensity show maximum at the surface plasmon resonance wavelength of 785 nm.

The black lines in Figure S15c,d show the calculated PT signal of a gold spheroid as a function of the wavelength of probe light according to eq 2 in the main text. The gold spheroid is 18 nm in length and 5 nm in diameter, which is placed on glass substrate and covered by PVA film. The rise of local temperature is fixed to be 5 K. The phase difference between the scattering field and the reference field in Figure S15c and S15d are $\phi_{\text{scat}} + 0.8\pi$ and $\phi_{\text{scat}} + 0.3\pi$, respectively.

In order to analyze the responses of the above four curves to the variation of local refractive index, we increased the refractive index of PVA by 0.1% and calculated the four curves again. The red lines in Figure S15 show the corresponding change rate which is defined as $(C_{\text{after}} - C_{\text{before}})/C_{\text{before}}$, where C_{before} and C_{after} are the calculated curves before and after the increase of the refractive index of PVA.

The change rates of the scattering spectrum (Figure S15a) and the absorption spectrum (Figure S15b) show nearly the same line shape. The maximal amplitudes of the change rate of the scattering spectrum and the absorption spectrum are both 3.05% occurred at the wavelength where the scattering and absorption intensity decrease to half of their maximum. The PT signal in Figure S15c shows symmetric peak at probe light wavelength of 785 nm. The amplitudes of the change rate are about 9.05% and 14.59% occurred at the wavelength where the PT signal decrease to half and quarter of the maximum, respectively, which are about 2.97 and 4.78 times higher than the maximal change rate in Figure S15a,b. The PT signal in Figure S15d shows anti-symmetric peak and valley at probe wavelength of 774 nm and 795 nm respectively. The amplitudes of the change rate are about 16.79% and 39.12% occurred at the wavelength where the PT signal decreases to half and quarter of the maximum, respectively, which are about 5.5 and 12.82 times higher than the maximal change rate in Figure S15a,b. Such huge response of the PT signal to the little variation of local refractive index could enable the sensing with ultra-high sensitivity in the fields of analytical chemistry and nanobiology.

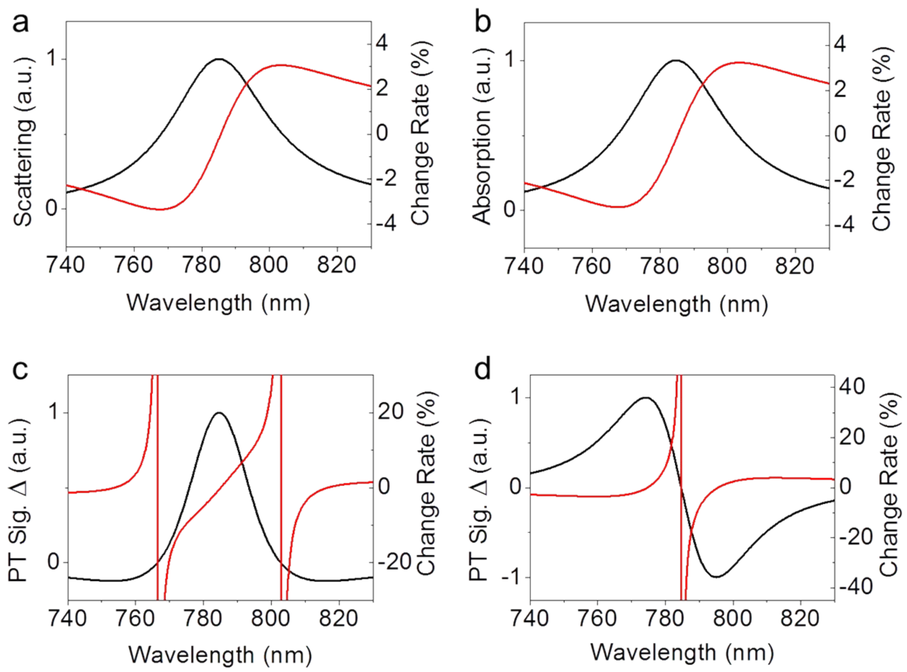

Figure S15. (a) Normalized scattering spectrum of gold spheroid (black line, left axis) and change rate of the scattering spectrum induced by the increase of refractive index of PVA by 0.1% (red line, right axis). (b) Normalized absorption spectrum of gold spheroid (black line, left axis) and change rate of the absorption spectrum induced by the increase of refractive index of PVA by 0.1% (red line, right axis). (c) PT signal of gold spheroid as a function of the probe light wavelength (black line, left axis) and change rate of the PT signal induced by the increase of refractive index of PVA by 0.1% (red lines, right axis). The rise of local temperature is fixed to be 5 K. The phase difference between the scattering field and the reference field is $\phi_{scat} + 0.8\pi$. (d) The same as (c) but for the phase difference between the scattering field and the reference field of $\phi_{scat} + 0.3\pi$.

REFERENCES

1. B. Nikoobakht and M. A. El Sayed, *Chem. Mater.*, 2003, **15**, 1957-1962.
2. P. B. Johnson and R. W. Christy, *Phys. Rev. B*, 1972, **6**, 4370-4379.
3. A. Gaiduk, P. V. Ruijgrok, M. Yorulmaz and M. Orrit, *Chem. Sci.*, 2010, **1**, 343.
4. M. Rashidi-Huyeh and B. Palpant, *Phys. Rev. B*, 2006, **74**, 075405.
5. J. Hwang and W. E. Moerner, *Opt. Commun.*, 2007, **280**, 487-491.
6. C. F. Bohren and D. R. Huffman, *Absorption and Scattering of Light by Small Particles*, John Wiley & Sons. Inc., New York, 1998.
7. S. Link, M. B. Mohamed and M. A. El-Sayed, *J. Phys. Chem. B*, 1999, **103**, 3073-3077.